Inorganic Chemistry
Article

Inorg. Chem. **2011**, *50*, 961–968 **961**
DOI: 10.1021/ic101562p

Copper(I) Coordination Polymers of *N,N′*-Bis[3-(methylthio)propyl]pyromellitic Diimide: Crystal Transformation and Solvatochromism by Halogen−π Interactions

Garam Park, Hojin Yang, Tae Ho Kim,* and Jineun Kim*

Department of Chemistry (BK21) and Research Institute of Natural Science, Gyeongsang National University, 900 Gajwa-dong, Jinju 660-701, South Korea

Received August 3, 2010

Four copper(I) coordination polymers with ligand *N,N′*-bis[3-(methylthio)propyl]pyromellitic diimide (**L**), $[Cu_2I_2L_2]_n$ (**1**), $[Cu_2I_2L_2]_n$ (**2**), $[Cu_2I_2L]_n$ (**3**), and $\{[Cu_2I_2L_2]\cdot CH_2Cl_2\}_n$ (**4**), have been successfully synthesized and structurally characterized by single-crystal X-ray diffraction. Structural transformations between the polymers were controlled by the appropriate solvent composition, mole ratio, or temperature. When a 1:1 CuI/**L** ratio was employed, dimorphic products, **1** and **2**, based on a rhomboid Cu_2I_2 cluster were obtained from an acetonitrile solution and from a dichloromethane/acetonitrile solution with ultrasonication, respectively. When a 1:2 CuI/**L** ratio was employed, polymer **3** based on infinite stair-step polymer $(CuI)_\infty$ was crystallized. Crystalline product **4** was obtained by the transformation of **1** in a mixed-solvent system with a 1:5 acetonitrile/dichloromethane ratio. Polymers **1**−**4** were transformed into polymer **3** at 197 °C. X-ray structures of **2**−**4** show short distances (3.406−3.667 Å) between halogens (I^- and Cl) and aromatic rings. **1** and **4** show solvatochromism; upon inclusion of the colorless electron donor CH_2Cl_2, the red color changes as a result of the formation of a chloride−π charge-transfer complex **4** of a pale-colored electron acceptor, **1**. Therefore, the origin of the red color from **2** and **3** is also assigned as iodide-to-electron-deficient aromatic π charge transfer.

Introduction

In recent years, copper(I) chemistry has attracted increasing attention because of the diverse structures and photophysical properties of the complexes[1] as well as potential applications such as electroluminescent displays.[2] Copper(I) complexes show unusually diverse geometries and stoichiometries of copper(I) halide clusters because of the relatively small energy difference between the various polymorphs, depending on the synthetic conditions such as the metal-to-ligand ratio and solvent. The structural diversity of these systems has provided an opportunity to understand the relationship between the photoluminescent properties and structures of these materials. Furthermore, considerable attention has been devoted to the rational synthesis of polymeric networks for copper(I) halide complexes based on nitrogen-donor ligands.[3] However, reports on polymeric copper(I) halide complexes of dithioether ligands are still sparse.[4] We have focused our interest on sulfur-donor ligands because the soft sulfur donor has an affinity for soft metals such as copper(I) or silver(I).[5] We examined the structural diversity of copper(I) halide complexes because of the structural modification of dithioether ligands by changing spacers between two sulfur atoms, such as piperazine, phenylene, and hydroquinone.[6] As part of our

*To whom correspondence should be addressed. E-mail: jekim@gnu.ac.kr (J.K.), thkim@gnu.ac.kr (T.H.K.). Tel.: +82-55-751-6024. Fax: +82-55-758-5532.

(1) (a) Peng, R.; Li, M.; Li, D. *Coord. Chem. Rev.* **2010**, *254*, 1. (b) Armaroli, N.; Accorsi, G.; Cardinali, F.; Listorti, A. *Top. Curr. Chem.* **2007**, *280*, 69. (c) Vitale, M.; Ford, P. C. *Coord. Chem. Rev.* **2001**, *219*−*221*, 3. (d) Ford, P. C.; Cariati, E.; Bourassa, J. *Chem. Rev.* **1999**, *99*, 3625.

(2) (a) Xia, H.; He, L.; Zhang, M.; Zeng, M.; Wang, X.; Lu, D.; Ma, Y. *Opt. Mater.* **2007**, *29*, 667. (b) Zhang, H.-Y.; Ye, K.-Q.; Zhang, J.-Y.; Liu, Y.; Wang, Y. *Inorg. Chem.* **2006**, *45*, 1745. (c) Jia, W. L.; McCormick, T.; Tao, Y.; Lu, J.-P.; Wang, S. *Inorg. Chem.* **2005**, *44*, 5706. (d) Zhang, Q.; Zhou, Q.; Cheng, Y.; Wang, L.; Ma, D.; Jing, X.; Wang, F. *Adv. Mater.* **2004**, *16*, 432.

(3) (a) Mukherjee, A.; Chakrabarty, R.; Patra, G. K. *Inorg. Chem. Commun.* **2009**, *12*, 1227. (b) Lee, Y.; Park, G. Y.; Lucas, H. R.; Vajda, P. L.; Kamaraj, K.; Vance, M. A.; Milligan, A. E.; Woertink, J. S.; Siegler, M. A.; Sarjeant, A. A. N.; Zakharov, L. N.; Rheingold, A. L.; Solomon, E. I.; Karlin, K. D. *Inorg. Chem.* **2009**, *48*, 11297. (c) Zhang, J.-X.; He, J.; Yin, Y.-G.; Hu, M.-H.; Li, D.; Huang, X.-C. *Inorg. Chem.* **2008**, *47*, 3471. (d) Tzeng, B.-C.; Chiu, T.-H.; Chen, B.-S.; Lee, G.-H. *Chem.—Eur. J.* **2008**, *14*, 5237.

(4) (a) Knorr, M.; Guyon, F.; Khatyr, A.; Daeschlein, C.; Strohmann, C.; Aly, S. M.; Abd-El-Aziz, A. S.; Fortin, D.; Harvey, D. P. *Dalton Trans.* **2009**, 948. (b) Xie, C.; Zhou, L.; Feng, W.; Wang, J.; Chen, W. *J. Mol. Struct.* **2009**, *921*, 132. (c) Peindy, H. N.; Guyon, F.; Khatyr, A.; Knorr, M.; Strohmann, C. *Eur. J. Inorg. Chem.* **2007**, 1823. (d) Romero, I.; Sanchez-Castello, G.; Teixidor, F.; Whitaker, C. R.; Rius, J.; Miravitlles, C.; Flor, T.; Escriche, L.; Casabo, J. *Polyhedron* **1996**, *15*, 2057.

(5) (a) Kim, T. H.; Shin, Y. W.; Jung, J. H.; Kim, J. S.; Kim, J. *Angew. Chem.* **2008**, *120*, 697. *Angew. Chem., Int. Ed.* **2008**, *47*, 685. (b) Seo, J.; Song, M. R.; Sultana, K. F.; Kim, H. J.; Kim, J.; Lee, S. S. *J. Mol. Struct.* **2007**, *827*, 201. (c) Kim, T. H.; Shin, Y. W.; Lee, S. S.; Kim, J. *Inorg. Chem. Commun.* **2007**, *10*, 11. (d) Kim, T. H.; Seo, J.; Park, K.-M.; Lee, S. S.; Kim, J. *Inorg. Chem. Commun.* **2007**, *10*, 313. (e) Seo, J.; Song, M. R.; Lee, J.-E.; Lee, S. Y.; Yoon, I.; Park, K.-M.; Kim, J.; Jung, J. H.; Park, S. B.; Lee, S. S. *Inorg. Chem.* **2006**, *45*, 952.

(6) (a) Kim, T. H.; Yang, H.; Park, G.; Lee, K. Y.; Kim, J. *Chem. Asian J.* **2010**, *5*, 252. (b) Kim, T. H.; Park, G.; Shin, Y. W.; Park, K.-M.; Choi, M. Y.; Kim, J. *Bull. Korean Chem. Soc.* **2008**, *29*, 499. (c) Kim, T. H.; Shin, Y. W.; Kim, J. S.; Lee, S. S.; Kim, J. *Inorg. Chem. Commun.* **2007**, *10*, 717.

Published on Web 12/28/2010

Scheme 1. Preparation of Coordination Polymers **1**−**4**

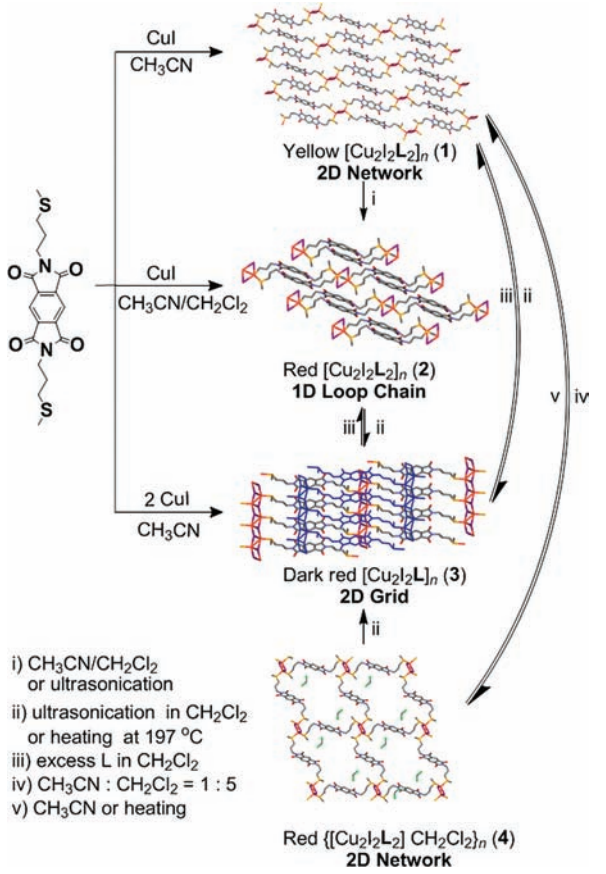

ongoing research, a pyromellitic diimide spacer was introduced into a dithioether ligand. Pyromellitic diimides were used as rigid structural components in catenanes and in supramolecular assemblies and acceptors in various electron-transfer and photosynthetic charge-separation systems.[7] Catenanes and supramolecular assemblies have led to the exploitation of many types of intermolecular interactions, including hydrogen-bonding, metal−ligand coordination, and anion−π interactions. One of the anion−π interactions, the halogen−π interaction, has garnered considerable attention because it plays an important role in the recognition of halides.[8] In this paper, we report on the synthesis and characterization of copper(I) coordination polymers (**1**−**4** in Scheme 1) of a dithioether ligand, *N*,*N*′-bis[3-(methylthio)propyl]pyromellitic diimide (**L**), and solvatochromism[9] by halogen−π charge-transfer (CT) interaction.

Experimental Section

General Methods. The ^{1}H and ^{13}C NMR spectra were recorded with a Bruker Advance-300 (300 MHz) NMR spectrometer. The Fourier transform IR spectra of the coordination polymers and ligand were measured with a Bruker Optics VERTEX 80v spectrometer. Elemental analysis was carried out on a CE EA1110 elemental analyzer. Thermogravimetric analysis (TGA) and differential thermal analysis (DTA) were performed under N_2(g) at a scan rate of 10 °C min^{-1} using a TA SDT Q600 thermal analyzer. For field-emission scanning electron microscopy (FE-SEM), compounds were placed on carbon tape after platinum coating, and the specimens were then examined with a JEOL JSM-6701F. Powder X-ray diffraction (PXRD) patterns were obtained with a Bruker AXS D8 DISCOVER diffractometer using Cu Kα (1.540 56 Å) radiation. Single-crystal X-ray diffraction data at low temperature were collected on Bruker SMART CCD and Bruker Ultra SMART CCD diffractometers (Central Laboratory, Gyeongsang National University, Jinju, South Korea) equipped with graphite-monochromated Mo Kα radiation (λ = 0.710 73 Å). The cell parameters for the compounds were obtained from a least-squares refinement of the spots using the *SMART* program. The intensity data were processed using the *SAINT Plus* program. All of the calculations for the structure determination were carried out using the *SHELXTL* package. Absorption corrections were applied by using the *SADABS* multiscan method. In most cases, hydrogen positions were input and refined in a riding manner along with the attached carbon atoms.

Synthesis of *N*,*N*′-Bis[(methylthio)propyl]pyromellitic Diimide (L). A mixture of pyromellitic dianhydride (1.09 g, 5.0 mmol) and 3-(methylthio)propylamine (1.05 g, 10.0 mmol) in toluene (1 mL) and quinoline (3 mL) was heated at 180 °C with stirring for 1 h. Upon cooling to room temperature, an off-white crude solid was filtered and washed with ether. A white powder was obtained. Yield: 74%. ^{1}H NMR (300 MHz, $CDCl_3$): δ 8.28 (s, 2H, Ar), 3.871 (t, 4H, NCH_2), 2.561 (t, 4H, SCH_2), 2.105 (s, 6H, SCH_3), 2.014 (m, 4H, CCH_2C). ^{13}C NMR (75.4 MHz, $CDCl_3$): δ 166.21, 137.25, 118.27, 37.76, 31.40, 27.46, 15.45. IR (KBr, ν, cm^{-1}): 3466 w, 3061 w, 3037 w, 2955 m, 2915 s, 2848 m, 1718 s, 1699 s, 1445 m, 1399 s, 1360 m, 1323 m, 1311 m, 1236 m, 1156 m, 1101 s, 1026 s, 992 m, 952 m, 916 m, 872 m, 833 w, 727 s, 559 s, 514 w. MS: *m*/*z* 392 (M, 44%), 345 (100), 317 (25), 297 (30), 270 (19), 87 (76).

[$Cu_2I_2L_2$]$_n$ (1). An acetonitrile (10 mL) solution of **L** (0.0196 g, 0.05 mmol) was allowed to mix with an acetonitrile (10 mL) solution of CuI (0.0095 g, 0.05 mmol). Yellow precipitates were filtered and washed with a 1:1 diethyl ether/acetonitrile solution (0.0280 g, 96.22%). Single crystals suitable for X-ray analysis were obtained by slow evaporation. IR (KBr, ν, cm^{-1}): 3466 w, 3095 w, 3035 w, 2984 w, 2939 w, 2922 w, 2865 w, 2819 w, 2510 w, 1771 s, 1710 s, 1565 w, 1450 m, 1435 m, 1431 m, 1395 s, 1371 s, 1358 s, 1352 s, 1337 m, 1308 m, 1242 w, 1196 w, 1158 w, 1129 w, 1120 s, 1016 s, 990 w, 954 w, 873 w, 832 m, 729 s, 622 w, 562 m. Anal. Calcd for $C_{36}H_{40}N_4O_8S_4Cu_2I_2$: C, 37.09; H, 3.46; N, 4.81; S, 11.00. Found: C, 36.52; H, 3.11; N, 5.00; S, 10.42.

[$Cu_2I_2L_2$]$_n$ (2). A dichloromethane (10 mL) solution of **L** (0.0196 g, 0.05 mmol) was allowed to mix with an acetonitrile (10 mL) solution of CuI (0.0095 g, 0.05 mmol), followed by ultrasonication. Red precipitates were filtered and washed with a 1:1 diethyl ether/acetonitrile solution (0.0210 g, 72.16%). Single crystals suitable for X-ray analysis were obtained by slow evaporation. IR (KBr, ν, cm^{-1}): 3466 w, 3090 w, 3023 w, 2941 w, 2910 w, 2831 w, 1768 s, 1716 s, 1696 s, 1459 m, 1440 m, 1426 m, 1395 s, 1366 s,

(7) (a) Kato, S.-i.; Nonaka, Y.; Shimasaki, T.; Goto, K.; Shinmyozu, T. *J. Org. Chem.* **2008**, *73*, 4063. (b) Jones, B. A.; Facchetti, A.; Wasielewski, M. R.; Marks, T. J. *J. Am. Chem. Soc.* **2007**, *129*, 15259. (c) Iwanaga, T.; Nakamoto, R.; Yasutake, M.; Takemura, H.; Sako, K.; Shinmyozu, T. *Angew. Chem.* **2006**, *118*, 3725. *Angew. Chem., Int. Ed.* **2006**, *45*, 3643. (d) Kato, S.-i.; Matsumoto, T.; Ideta, K.; Shimasaki, T.; Goto, K.; Shinmyozu, T. *J. Org. Chem.* **2006**, *71*, 4723. (e) Wiederrecht, G. P.; Svec, W. A.; Wasielewski, M. R.; Galili, T.; Levanon, H. *J. Am. Chem. Soc.* **2000**, *122*, 9715.

(8) (a) Hay, B. P.; Custelcean, R. *Cryst. Growth Des.* **2009**, *9*, 2539. (b) Han, B.; Lu, J.; Kochi, J. K. *Cryst. Growth Des.* **2008**, *8*, 1327. (c) Hay, B. P.; Bryantsev, V. S. *Chem. Commun.* **2008**, 2417. (d) Lu, Y.-X.; Zou, J.-W.; Wang, Y.-H.; Yu, Q.-S. *Chem. Phys.* **2007**, *334*, 1. (e) Berryman, O. B.; Bryantsev, V. S.; Stay, D. P.; Johnson, D. W.; Hay, B. P. *J. Am. Chem. Soc.* **2007**, *129*, 48. (f) Lu, Y.-X; Zou, J.-W.; Wang, Y.-H.; Yu, Q.-S. *Int. J. Quantum Chem.* **2007**, *107*, 1479. (g) Gamez, P.; Mooibroek, T. J.; Teat, S. J.; Reedijk, J. *Acc. Chem. Res.* **2007**, *40*, 435. (h) Rosokha, Y. S.; Lindeman, S. V.; Rosokha, S. V.; Kochi, J. K. *Angew. Chem.* **2004**, *35*, 4750. *Angew. Chem., Int. Ed.* **2004**, *43*, 4650. (i) Mascal, M.; Armstrong, A.; Bartberger, M. D. *J. Am. Chem. Soc.* **2002**, *124*, 6274. (j) Quiñonero, D.; Garau, C.; Rotger, C.; Frontera, A.; Ballester, P.; Costa, A.; Deyà, P. M. *Angew. Chem.* **2002**, *114*, 3539. *Angew. Chem., Int. Ed.* **2002**, *41*, 3389. (k) Alkorta, I.; Rozas, I.; Elguero, J. *J. Org. Chem.* **1997**, *62*, 4687.

(9) (a) Cariati, E.; Bourassa, J.; Ford, P. C. *Chem. Commun.* **1998**, 1623. (b) Cariati, E.; Bu, X.; Ford, P. C. *Chem. Mater.* **2000**, *12*, 3385.

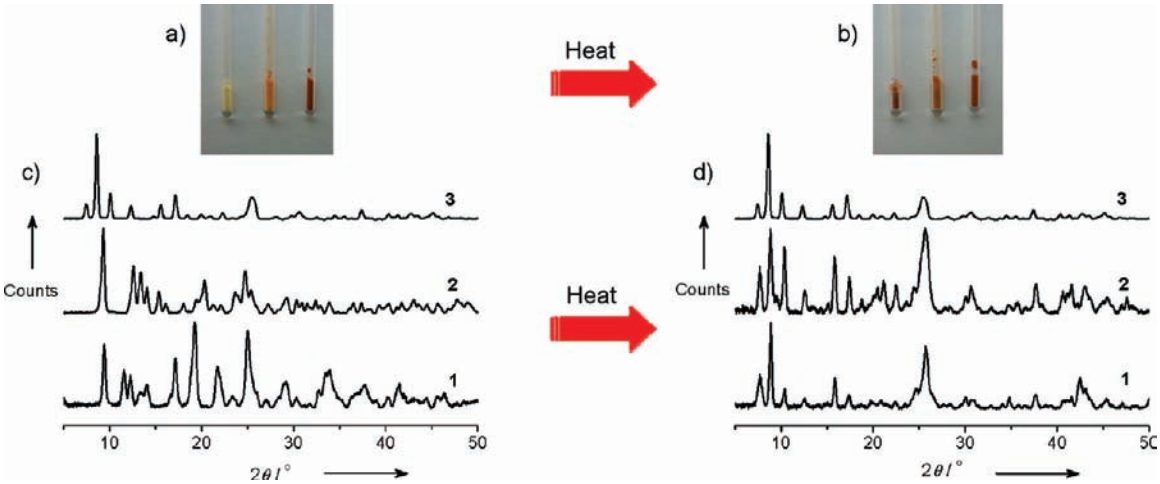

Figure 1. Photographs of **1**−**3** before (a) and after (b) heating. PXRD patterns of **1**−**3** before (c) and after (d) heating.

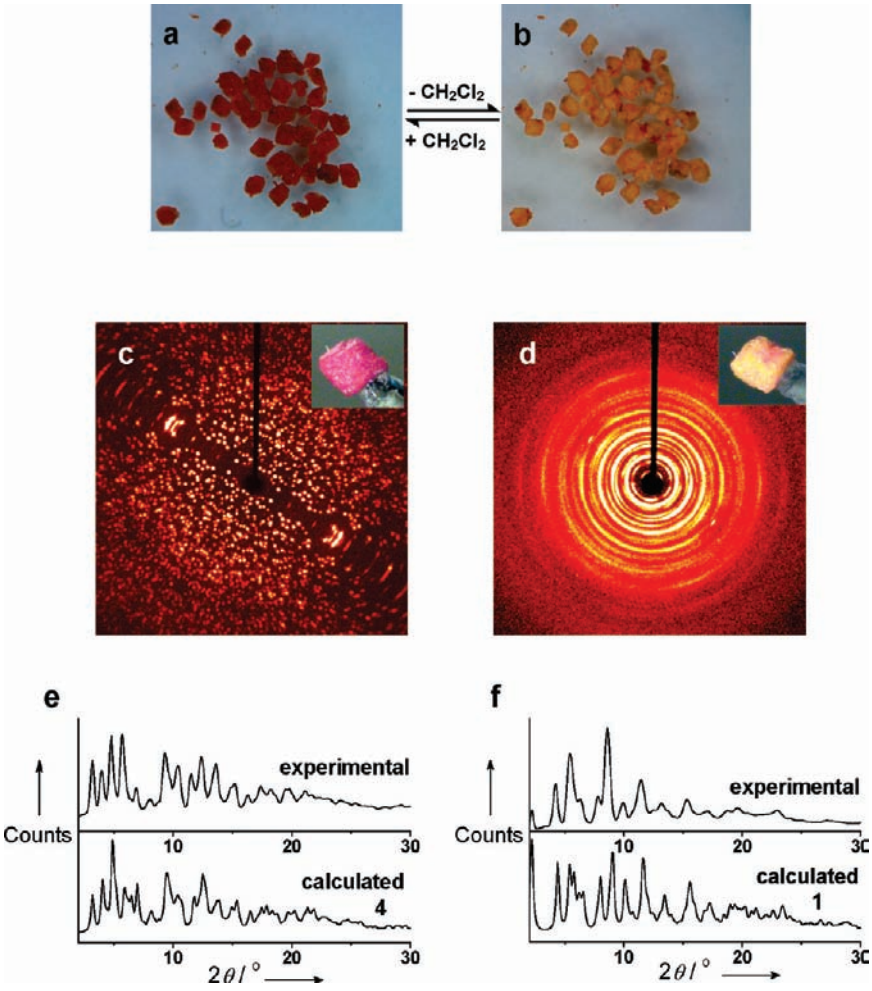

Figure 2. Photograph of crystal **4** before (a) and after (b) heating: yellow crystals are contaminated by a small amount of red crystal **3**, and red crystal **4** was reformed by exposure of CH_2Cl_2 to **1** in 1:5 CH_3CN/CH_2Cl_2. Photographs and X-ray diffraction frame images of a single crystal **4** before (c) and after (d) heating. X-ray diffraction patterns of **4** before (e) and after (f) heating.

1354 s, 1292 w, 1227 m, 1155 w, 1122 m, 1093 m,1072 w, 1057 w, 1026 s, 968 w, 880 w, 854 w, 794 w, 727 s, 607 w, 598 w, 561 m. Anal. Calcd for $C_{36}H_{40}N_4O_8S_4Cu_2I_2$: C, 37.09; H, 3.46; N, 4.81; S, 11.00. Found: C, 36.82; H, 3.21; N, 4.80; S, 10.82.

$[Cu_2I_2L]_n$ (3). A dichloromethane (20 mL) solution of **L** (0.0392 g, 0.10 mmol) was allowed to mix with an acetonitrile (30 mL) solution of CuI (0.0190 g, 0.10 mmol), followed by ultrasonication. Red precipitates were filtered and washed with a 1:1 diethyl ether/acetonitrile solution (0.0526 g, 90.38%). IR (KBr, ν, cm^{-1}): 3456 w, 3023 w, 2941 w, 2920 w, 1766 m, 1706 s, 1696 s, 1457 m, 1426 m, 1402 s, 1368 s, 1335 m, 1218 m, 1158 m, 1124 m, 1103 m, 1036 s, 926 w, 851 m, 787 w, 727 s, 610 m, 559 m. Anal. Calcd for $C_{18}H_{20}N_2O_4S_2Cu_2I_2$: C, 27.95; H, 2.61; N, 3.62. Found: C, 28.06; H, 2.27; N, 3.55.

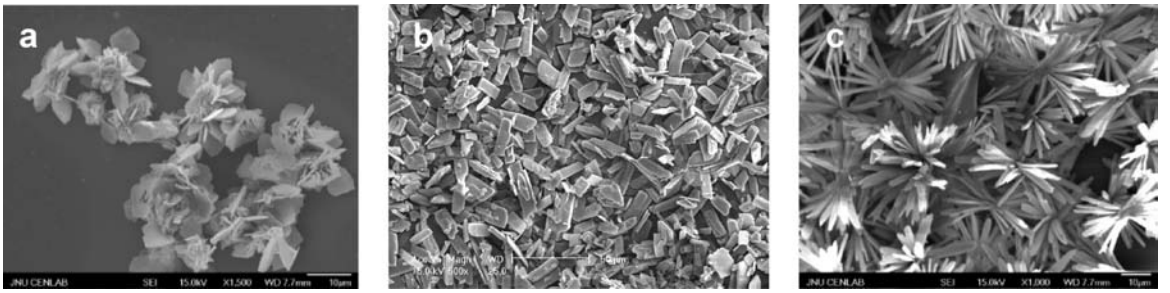

Figure 3. SEM images of **1**−**3**: rose-shaped sheet **1** (a); plate-shaped **2** (b); needle-shaped **3** (c).

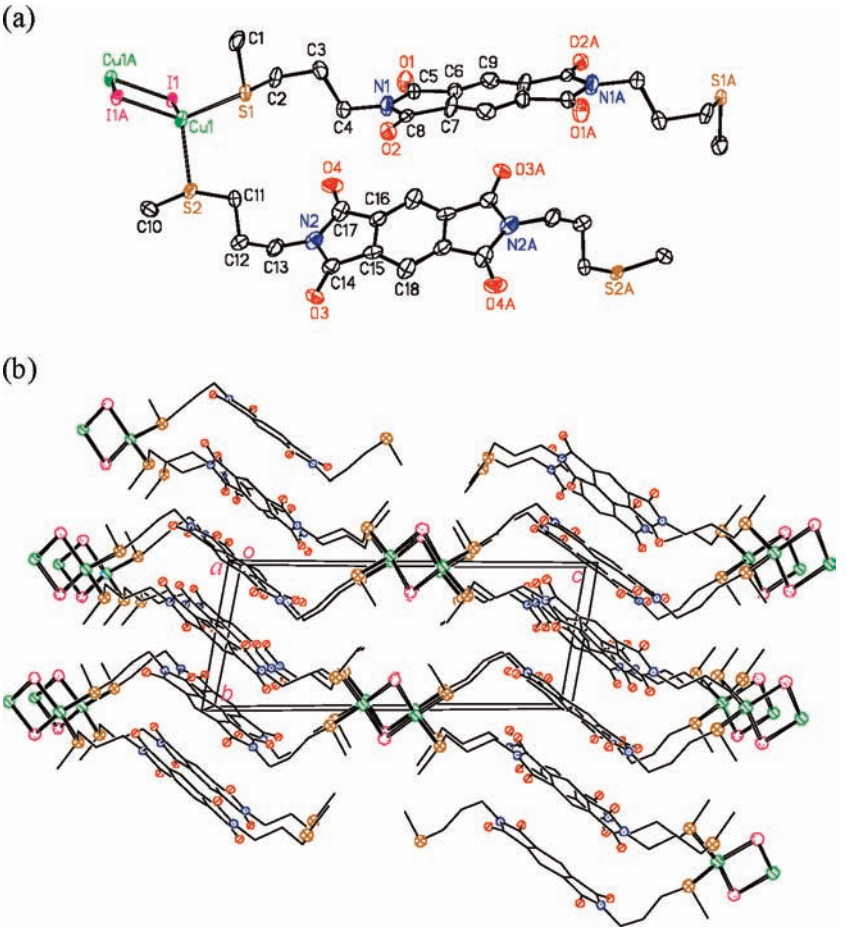

Figure 4. ORTEP drawing (a) with thermal ellipsoids drawn at the 50% probability level and a packing diagram (b) of **1** (C, gray; N, blue; O, red; S, yellow; Cu, green; I, purple). Hydrogen atoms are omitted.

$\{[Cu_2I_2L_2]\cdot CH_2Cl_2\}_n$ **(4).** Yellow powder (**1**) was immersed in a mixed solvent of 1 mL of acetonitrile and 5 mL of dichloromethane, and the resulting mixture left for a few weeks at room temperature. Single crystals suitable for X-ray analysis were obtained. IR (KBr, ν, cm^{-1}): 3097 w, 3035 w, 2992 w, 2915 w, 1769 m, 1709 s, 1436 w, 1395 m, 1369 m, 1352 m, 1309 w, 1239 w, 1158 w, 1103 w, 1017 w, 876 w, 830 w, 727 m, 562 w.

Results and Discussion

Synthesis and Crystal Transformation. The ligand **L** was synthesized from pyromellitic anhydride and 3-(methylthio)-propylamine using a similar method in the literature.[10] A self-assembly reaction between CuI and **L** afforded four coordination polymers, yellow (**1**) and red (**2**, **3**, and **4**) compounds, under appropriate synthetic conditions (Scheme 1). The rapid mixing of acetonitrile solutions of CuI and **L** in a 1:1 mole ratio yielded polymer **1**, indicating that **1** is kinetically stable. Polymer **2** was prepared by the mixing of an acetonitrile solution of CuI and a dichloromethane solution of **L** in a 1:1 mole ratio, followed by ultrasonication. Polymer **3** was obtained by the mixing of acetonitrile solutions of CuI and **L** in a 2:1 mole ratio. Conversion between **1**−**4** was controlled by the appropriate solvent composition, mole ratio, or temperature (Scheme 1).[11] In most cases, polymer **1** was transformed into polycrystalline **2** by ultrasonication in

(10) (a) Yeganeh, H.; Barikani, M. *Polym. Int.* **2000**, *49*, 514. (b) Nielsen, M. B.; Hansen, J. G.; Becher, J. *Eur. J. Org. Chem.* **1999**, 2807.

(11) (a) Jess, I.; Taborsky, P.; Pospisil, J.; Naether, C. *Dalton Trans.* **2007**, 2263. (b) Cariati, E.; Roberto, D.; Ugo, R.; Ford, P. C.; Galli, S.; Sironi, A. *Chem. Mater.* **2002**, *14*, 5116.

Table 1. Crystallographic Data and Structural Refinement for **1**−**4**

	$[Cu_2I_2\mathbf{L}_2]_n$ (**1**)	$[Cu_2I_2\mathbf{L}_2]_n$ (**2**)	$[Cu_2I_2\mathbf{L}]_n$ (**3**)	$\{[Cu_2I_2\mathbf{L}_2]\cdot CH_2Cl_2\}_n$ (**4**)
empirical formula	$C_{18}H_{20}N_2O_4S_2CuI$	$C_{18}H_{20}N_2O_4S_2CuI$	$C_{18}H_{20}N_2O_4S_2Cu_2I_2$	$C_{19}H_{22}N_2O_4S_2CuI$
fw	582.92	582.92	773.36	667.85
color	yellow	red	dark red	red
T (K)	173(2)	173(2)	173(2)	173(2)
wavelength (Å)	0.710 73	0.710 73	0.710 73	0.710 73
cryst syst	triclinic	triclinic	triclinic	triclinic
space group	$P\bar{1}$	$P\bar{1}$	$P\bar{1}$	$P\bar{1}$
a (Å)	7.2384(14)	9.5404(8)	4.4520(4)	9.4682(7)
b (Å)	7.7561(15)	11.0627(9)	10.5759(9)	10.0563(7)
c (Å)	19.188(4)	11.2515(9)	12.2370(11)	13.0343(9)
α (deg)	100.062(11)	62.3060(10)	100.1480(10)	88.6690(10)
β (deg)	99.706(10)	82.8810(10)	92.6900(10)	78.3370(10)
γ (deg)	90.402(10)	83.9750(10)	96.8260(10)	87.5330(10)
volume (Å^3)	1044.7(4)	1041.85(15)	561.77(9)	1214.18(15)
Z	2	2	1	2
D_{calcd} (Mg m^{-3})	1.853	1.858	2.286	1.827
abs coeff (mm^{-1})	2.750	2.757	4.855	2.591
F(000)	576	576	370	660
cryst size (mm^3)	0.12 × 0.09 × 0.03	0.30 × 0.20 × 0.10	0.30 × 0.20 × 0.10	0.35 × 0.25 × 0.15
θ range (deg)	2.19−27.00	2.15−27.00	1.69−27.00	1.60−27.00
index ranges	$-9 \le h \le +9$	$-12 \le h \le +12$	$-5 \le h \le +5$	$-12 \le h \le +12$
	$-9 \le k \le +9$	$-14 \le k \le +14$	$-13 \le k \le +13$	$-12 \le k \le +9$
	$-24 \le l \le +24$	$-14 \le l \le +14$	$-15 \le l \le +15$	$-16 \le l \le +16$
no. of reflns collected	16 887	9085	4857	7519
no. of indep reflns	4538	4485	2414	5146
	R_{int} = 0.0478	R_{int} = 0.0220	R_{int} = 0.0213	R_{int} = 0.0176
no. of data/restraints/params	4538/0/255	4485/0/255	2414/0/137	5146/0/301
GOF on F^2	1.097	1.049	1.288	1.108
final R indices [$I > 2\sigma(I)$]	R1 = 0.0647, wR2 = 0.1811	R1 = 0.0223, wR2 = 0.0555	R1 = 0.0225, wR2 = 0.0623	R1 = 0.0283, wR2 = 0.0702
R indices (all data)	R1 = 0.0798, wR2 = 0.1876	R1 = 0.0301, wR2 = 0.0577	R1 = 0.0253, wR2 = 0.0784	R1 = 0.0402, wR2 = 0.0826
CCDC	778502	778503	778504	778505

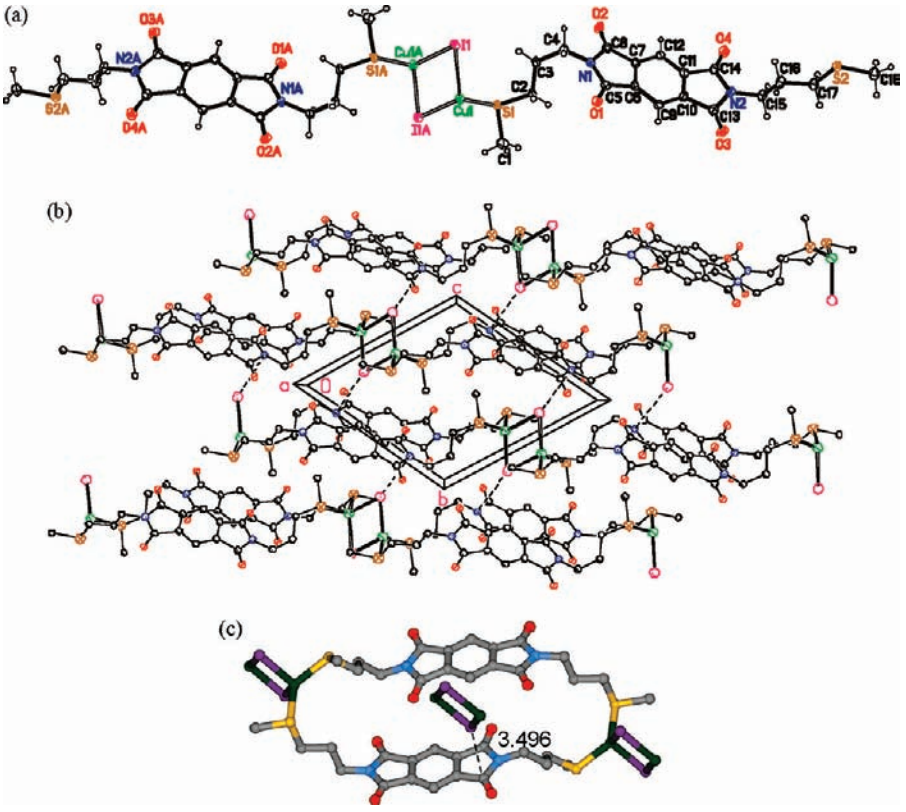

Figure 5. ORTEP drawing (a) with thermal ellipsoids drawn at the 50% probability level and a packing diagram (b) and a view (c) of **2** showing I$^-$−π interaction (C, gray; N, blue; O, red; S, yellow; Cu, green; I, purple). Hydrogen atoms are omitted.

CH_3CN/CH_2Cl_2, and then the slow evaporation of dichloromethane yielded good single crystals (i in Scheme 1). Polymer **1** was transformed into **3** by the addition of excess CuI. Also, **1** yielded polycrystalline **3** in CH_2Cl_2 after ultrasonication

(ii in Scheme 1). Conversely, single crystals of **3** and free **L** were obtained when **1** and its mother liquor were left for a few days. When **L** was added to **3** in the presence of solvent, **3** was transformed into mixed crystals, **1** and **2** (iii in Scheme 1). Dark-red **3** was also obtained by heating **1** and **2** at 197 °C without solvent (Figure 1). This implies that **3** is thermodynamically most stable at high temperatures. PXRD patterns for **1**−**3** before and after heating are shown in parts c and d of Figure 1, respectively. PXRD patterns after the heating of **1**−**3** at 197 °C are the same as that of **3**. Crystal **4** was transformed into **3** via **1** by heating it at 197 °C.

Complex **4** was prepared by the slow conversion of **1** in 1:5 CH_3CN/CH_2Cl_2 (iv in Scheme 1). At room temperature, red polymer **4** (Figure 2a) slowly lost dichloromethane solvates, leaving **1**. Crystal **4** was shortly transformed into **1** by heating it at a range of 40−120 °C (Figure 2b and v in Scheme 1). The PXRD pattern of the heated sample is the same as the simulated PXRD pattern of **1** (Figure 2). Red crystal **4** was reformed by exposure of CH_2Cl_2 to **1** in 1:5 CH_3CN/CH_2Cl_2: upon inclusion of a colorless electron donor CH_2Cl_2 (or I^- for **2** and **3**), the color changes as a result of the formation of CT complexes of a pale-colored electron acceptor, pyromellitic diimide. These processes were reversible (Figure 2). This is an example of solvatochromism by halogen (e.g., chlorine)−π interaction. Unfortunately, solvatochromism was not observed for some other halogen compounds including chloroform and highly toxic carbon tetrachloride. Probably, the volume of chloroform or carbon tetrachloride differs from the space occupied by dichloromethane in compound **4**.

Electron Microscophy. Figure 3 shows SEM images of the microsized powders of **1**−**3**. The morphology of **1** looks like rose flowers, as shown in Figure 3a, which were composed of very thin sheets. The image of **2** shows that **2** was precipitated as single-crystal-like plates. Polymer **3** was obtained as needle crystals, like pine needles. The images indicate that all samples were composed of homogeneous crystals in morphology. They were chemically pure and yielded good elemental analysis data and PXRD patterns, which agree with simulated PXRD patterns.

X-ray Crystallography. In yellow **1** with the formula $[Cu_2I_2\mathbf{L}_2]_n$, the packing structure is a brick-wall-type two-dimensional (2D) network with rhomboid Cu−I_2−Cu nodes (Figure 4 and Table 1). In the asymmetric unit of crystal **1**, a copper atom, one iodide ion, and each half of two ligands are unique. Inversion centers are located on the center of the aromatic rings and rhomboid Cu−I_2−Cu nodes. A layer of the network is packed repeatedly over another layer along the crystallographic *a* axis. There is no interaction between the iodide ions and the pyromellitic diimides; thus, **1** is pale-yellow, as are most d^{10} copper(I) complexes. The coordination environment of copper(I) has distorted tetrahedral geometry with two μ_2-bridge iodine atoms and two sulfur-donor atoms.

Compound **2** is dimorphic with **1** because their formulas are $[Cu_2I_2\mathbf{L}_2]_n$. The asymmetric unit consists of a copper ion, one iodine ion, and one ligand. Inversion centers are located on the center of the rhomboid Cu−I_2−Cu nodes. Structural analysis of **2** reveals one-dimensional (1D) loop chains with Cu−I_2−Cu nodes (Figure 5 and Table 1). Polymer **2** has a staggered arrangement of adjacent chains because the adjacent chains are shifted by half of the repeated loop unit

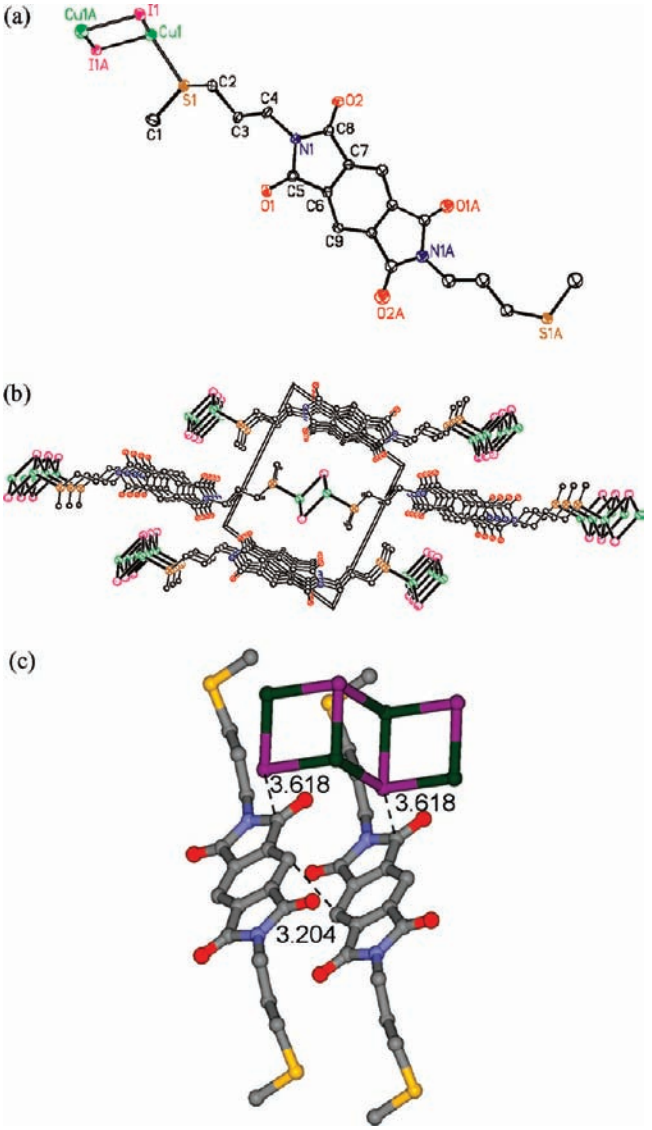

Figure 6. ORTEP drawing (a) with thermal ellipsoids drawn at the 50% probability level and a packing diagram (b) and a view (c) of **3** showing I^-−π and π−π interactions (C, gray; N, blue; O, red; S, yellow; Cu, green; I, purple). Hydrogen atoms are omitted.

along the crystallographic [0$\bar{2}$2] direction. Thus, iodide ions interact with the π electrons of pyromellitic diimides. The interaction distance between an iodide and a carbon is 3.496(2) Å (Figure 5c). In contrast to planar pyromellitic diimides of **1**, **3**, and **4**, pyromellitic diimides in **2** have a bent shape and nitrogen atoms are located 0.185(4) and 0.196(3) Å above mean benzene plane.

In the asymmetric unit of crystal **3**, a copper atom, one iodide ion, and half a ligand are unique. Inversion centers are located on the center of the aromatic rings and on the middle of the copper−copper lines (e.g., Cu1−Cu1A) in stairs. The crystal structure of **3**, $[Cu_2I_2\mathbf{L}]_n$, is a 2D grid (Figure 6 and Table 1). Each tetrahedral copper(I) ion is coordinated by three μ_3-I ligands, which generates a polymeric CuI 1D staircase. All 1D CuI staircases are aligned parallel to the *a* axis along the line crossing crystallographic (011) and (0$\bar{1}$1) planes. The ligands link copper(I) ions between 1D polymeric CuI staircases, and the structure becomes a 2D layer. Neighboring layers are shifted by half a layer, so layers are packed in an ABA-

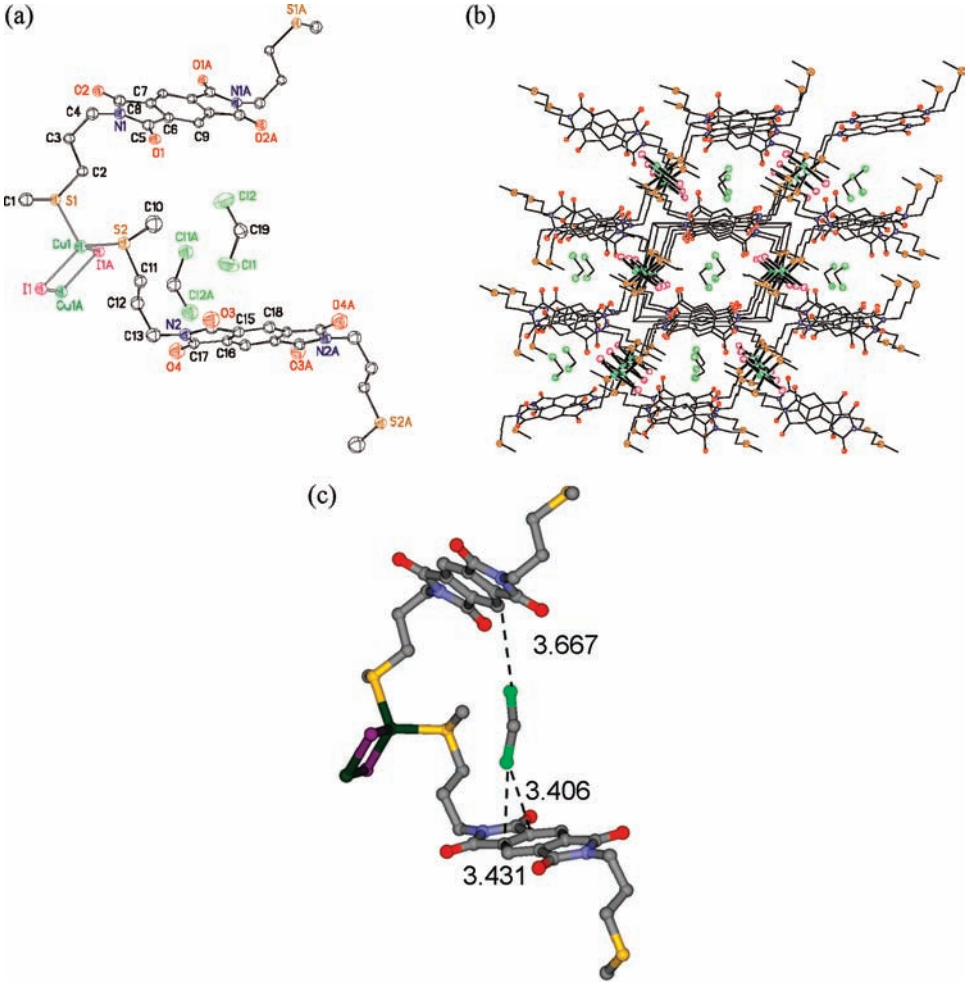

Figure 7. ORTEP drawing (a) with thermal ellipsoids drawn at the 50% probability level and a packing diagram (b) and a view (c) of **4** showing Cl$-\pi$ interaction (C, gray; N, blue; O, red; S, yellow; Cu, green; I, purple; Cl, light green). Hydrogen atoms are omitted.

BAB manner. Hence, iodide ions are in close contact with π electrons of the pyromellitic diimides [3.618(4) Å; Figure 8b]. In addition to halogen$-\pi$ interaction, $\pi-\pi$ stacking interactions between carbon atoms of the pyromellitic diimides [3.204(5) Å] stabilize crystal packing.

The crystal structure of **4**, $\{[Cu_2I_2L_2]\cdot 2CH_2Cl_2\}_n$, is also a brick-wall-type 2D network with rhomboid Cu$-I_2-$Cu nodes like **1** except with cavities for dichloromethane solvates (Figure 7 and Table 1). The asymmetric unit of crystal **4** is composed of a copper atom, one iodide ion, and each half of two ligands. Inversion centers are located on the center of the aromatic rings and Cu$-I_2-$Cu nodes. Solvate dichloromethane molecules are located in channels parallel to the crystallographic *b* axis. The chloride atoms of dichloromethane are in short contact with the carbon atoms [3.406(3), 3.431(3), and 3.667(3) Å] of the pyromellitic diimides (Figure 7c).

Thermoanalytical Investigations. To investigate the thermal stabilities of **1**$-$**4**, TGA and DTA were carried out at a rate of 10 °C/min in a N_2 atmosphere (Figure 8). All TGA curves exhibit very similar weight loss patterns in the range of 230$-$400 °C, which correspond to the decomposition and removal of **L**. The TGA curve of **4** shows the removal of solvate CH_2Cl_2 in temperatures ranging from 40 to 120 °C. DTA curves of **1**, **2**, and **4** show two peaks at 197 and 266 °C. The peak at 197 °C is an

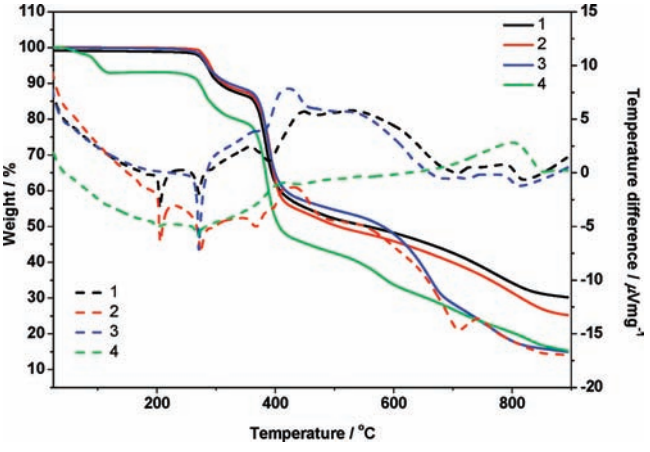

Figure 8. TGA (solid lines) and DTA (dashed lines) traces of **1**$-$**4**.

important indication for crystal transformation from **1**, **2**, and **4** to **3**, which is not accompanied by a significant weight loss. PXRD data prove that the products of these transformations are the same as **3** (Figure 1). The endothermic DTA signals at 266$-$268 °C correspond to the energy required for the decomposition and removal of **L**.

Diffuse Reflectance Spectra. The UV$-$vis spectrum of **1** shows a broad reflectance band in most visible regions

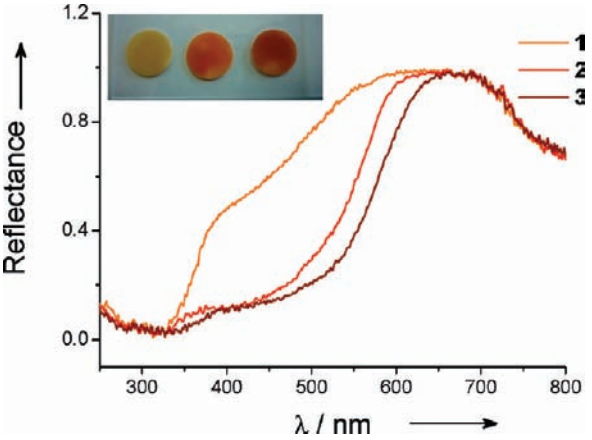

Figure 9. Solid-state reflectance UV−Vis spectra of **1**−**3**.

and some absorption in the blue region (Figure 9). The polymers **2** and **3** show strong reflection in the red region. These observations are in good agreement with the observed yellow, bright-red, and dark-red colors for **1**−**3**, respectively. In contrast to common pale-colored copper(I) complexes with d^{10} electronic configuration, the red colors for **2**−**4** are explained by CT from halogen to electron-deficient pyromellitic diimide as mentioned above: as shown in Figures 5−7, the halides lie 3.406−3.618 Å over the periphery of the aromatic ring. These compounds are nonluminescent. Although most copper(I) compounds show photoluminescent properties, rhomboid Cu_2I_2 complexes with only sulfur-donor ligands did not emit visible light under UV irradiation.[5c,6b]

In the present work, four coordination polymers based on CuI and **L** were investigated. Crystal transformation by heat, mole ratio, and solvent has been demonstrated. Iodide anion−π and chloride−π interactions have been observed. The recognition of halogen compounds by electron-deficient aromatic π acceptors is visually apparent by the color resulting from the diagnostic CT. Thus, halogen−π interactions could be used for the design and construction of sensors to detect environmentally hazardous halogen compounds with the naked eye.

Acknowledgment. This research was supported by the Basic Science Research Program through the National Research Foundation of Korea (NRF), funded by the Ministry of Education, Science and Technology (Grant 2010-0016386).

Supporting Information Available: Crystallographic information file, ORTEP diagram of **L**, crystal data and structure refinement for **L**, and experimental and simulated PXRD patterns for **1**−**3**. This material is available free of charge via the Internet at http://pubs.acs.org.